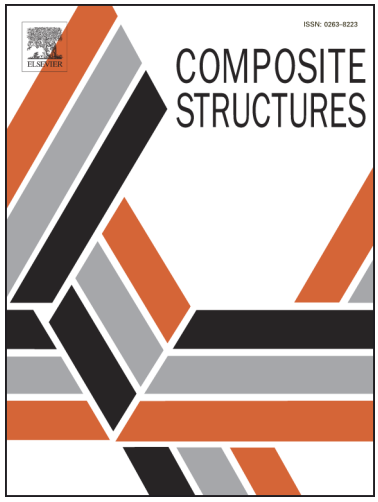

Size-dependent behaviour of functionally graded sandwich microbeams based on the modified couple stress theory

Huu-Tai Thai, Thuc P. Vo, Trung-Kien Nguyen, Jaehong Lee

PII: S0263-8223(14)00646-1
DOI: http://dx.doi.org/10.1016/j.compstruct.2014.11.065
Reference: COST 6050

To appear in: *Composite Structures*

Please cite this article as: Thai, H-T., Vo, T.P., Nguyen, T-K., Lee, J., Size-dependent behaviour of functionally graded sandwich microbeams based on the modified couple stress theory, *Composite Structures* (2014), doi: http://dx.doi.org/10.1016/j.compstruct.2014.11.065

Size-dependent behaviour of functionally graded sandwich microbeams based on the modified couple stress theory

Huu-Tai Thai [a,*], Thuc P. Vo [b], Trung-Kien Nguyen [c], Jaehong Lee [d]

[a] Centre for Infrastructure Engineering and Safety, School of Civil and Environmental Engineering, The University of New South Wales, Sydney, NSW 2052, Australia

[b] Faculty of Engineering and Environment, Northumbria University, Newcastle upon Tyne NE1 8ST, UK

[c] Faculty of Civil Engineering and Applied Mechanics, University of Technical Education Ho Chi Minh City, 1 Vo Van Ngan Street, Thu Duc District, Ho Chi Minh City, Vietnam

[d] Department of Architectural Engineering, Sejong University, 98 Kunja Dong, Kwangjin Ku, Seoul 143-747, Korea

Abstract

Static bending, buckling and free vibration behaviours of size-dependent functionally graded (FG) sandwich microbeams are examined in this paper based on the modified couple stress theory and Timoshenko beam theory. To avoid the use of a shear correction factor, equilibrium equations were used to compute the transverse shear force and shear stress. Two types of sandwich beams were considered: (1) homogeneous core and FG skins and (2) FG core and homogeneous skins. Numerical results were presented to illustrate the small scale effects on the behaviours of FG sandwich beams. The results reveals that the inclusion of the size effects results in an increase in the beam stiffness, and consequently, leads to a reduction of deflections and stresses and an increase in natural frequencies and critical buckling loads. Such effects are more pronounced when the beam depth was small, but they become negligible with the increase of the beam depth.

Keywords: Functionally graded sandwich beam; small scale effect; modified couple

[*] Corresponding author. Tel.: + 61 2 9385 5029.
E-mail address: t.thai@unsw.edu.au (H.T. Thai)

stress theory; Timoshenko beam

1. Introduction

Sandwich structures have been widely used in automotive, marine and aerospace industries due to their high strength-to-weight ratio. Conventional sandwich structures composed of a soft core bonded to two thin and stiff skins exhibit the delamination problems at the bond interfaces due to the sudden change in material properties between layers. To overcome this problem, functionally graded (FG) sandwich structures were proposed in which the core or two skins can be made from functionally graded materials (FGMs). The FGM is a kind of advanced composites in which its material properties vary smoothly from one surface to another, and thus eliminating the stress concentration found in laminated composites.

The application of FGMs in micro- and nano-scale devices and systems such as thin films [1], atomic force microscopes [2], micro- and nano-electro-mechanical systems (MEMS and NEMS) [3] has been increasingly in recent years. In such applications, size effects were experimentally observed [4-6]. The size effect can be captured using size-dependent continuum theories. In view of the difficulties in determining the material length scale parameters, Yang et al. [7] proposed the modified couple stress theory in which only one length scale parameter is required. There have been a number of size-dependent models developed for FG beams based on the modified couple stress theory [8-18]. These size-dependent models adopted various beam theories such as Euler-Bernoulli beam theory (EBT) [8-11], Timoshenko beam theory (TBT) [9-10, 12-14], and higher-order shear deformation beam theory (HBT) [10, 15-18]. It is worth noting that the EBT is the simplest one but it neglects the shear deformation effect which is significant in advanced composites like FGMs. The TBT accounts for the shear

deformation effect but it requires a shear correction factor which is hard to determine consistently. Although the HBTs do account for the shear deformation effect without requiring the shear correction factor, their equations of motion are more complicated than those of the TBT.

Although the size-dependent beam models based on the modified couple stress theory have been developed and well discussed in the above-mentioned studies for FG beams, no literature has been reported for the size-dependent behaviours of FG sandwich beams. This paper therefore aims to investigate the size-dependent behaviours of FG sandwich beams based on the modified couple stress theory and the TBT. To avoid the use of a shear correction factor in the Timoshenko beam theory, equilibrium equations were used to compute the transverse shear force and shear stress. FG sandwich beams with either two skins or a core made of FGMs were considered in this study. Numerical examples for simply supported beams were presented to investigate the influences of small scale on deflections, stresses, critical buckling loads and natural frequencies of FG sandwich beams.

2. Theoretical formulation

In this section, the formulations of a size-dependent FG sandwich beam model were briefly presented. The effects of the small scale and shear deformation were respectively accounted for using the modified couple stress theory and Timoshenko beam theory. Analytical solutions of simply supported beams were also presented using Navier-type solutions.

2.1. Governing equations of motion

In the modified couple stress theory, the strain energy is expressed in terms of both strain tensor and curvature tensor as [7]:

$$U = \frac{1}{2}\int_V \left(\sigma_{ij}\varepsilon_{ij} + m_{ij}\chi_{ij}\right) dV \tag{1}$$

where σ_{ij} and ε_{ij} are the components of the stress tensor and strain tensor; m_{ij} and χ_{ij} denote the components of the deviatoric part of the symmetric couple stress tensor and symmetric curvature tensor defined by:

$$m_{ij} = 2G\ell^2\chi_{ij}, \quad i, j = 1, 2, 3 \tag{2}$$

$$\chi_{ij} = \frac{1}{2}\left(\frac{\partial\theta_i}{\partial x_j} + \frac{\partial\theta_j}{\partial x_i}\right), \quad i, j = 1, 2, 3 \tag{3}$$

where G is the shear modulus; ℓ is the material length scale parameter accounting for the effect of the couple stress; and θ_i are the components of the rotation vector related to the displacement field (u_1, u_2, u_3) as:

$$\theta_x = \theta_1 = \frac{1}{2}\left(\frac{\partial u_3}{\partial x_2} - \frac{\partial u_2}{\partial x_3}\right) \tag{4a}$$

$$\theta_y = \theta_2 = \frac{1}{2}\left(\frac{\partial u_1}{\partial x_3} - \frac{\partial u_3}{\partial x_1}\right) \tag{4b}$$

$$\theta_z = \theta_3 = \frac{1}{2}\left(\frac{\partial u_2}{\partial x_1} - \frac{\partial u_1}{\partial x_2}\right) \tag{4c}$$

According to the Timoshenko beam theory, the displacement field is given by:

$$\begin{aligned} u_1(x, z, t) &= u(x, t) + z\varphi(x, t) \\ u_2(x, z, t) &= 0 \\ u_3(x, z, t) &= w(x, t) \end{aligned} \tag{5}$$

where u and w are the axial and transverse displacements of a point on the midplane of the beam; and φ is the rotation of the cross section. The nonzero components of linear strain and curvature in view of the displacement field in Eq. (5) are:

$$\varepsilon_{xx} = \frac{du}{dx} + z\frac{d\varphi}{dx} \tag{6a}$$

$$\gamma_{xz} = \varphi + \frac{dw}{dx} \tag{6b}$$

$$\chi_{xy} = \frac{1}{4}\left(\frac{d\varphi}{dx} - \frac{d^2w}{dx^2}\right) \tag{6c}$$

Using Hamilton's principle, the governing equations of motion are obtained as [9]:

$$\delta u: \ \frac{dN}{dx} = I_0\ddot{u} + I_1\ddot{\varphi} \tag{7a}$$

$$\delta w: \frac{dQ}{dx} + \frac{1}{2}\frac{d^2Y}{dx^2} - P_0\frac{d^2w}{dx^2} + q = I_0\ddot{w} \tag{7b}$$

$$\delta\varphi: \ \frac{dM}{dx} - Q + \frac{1}{2}\frac{dY}{dx} = I_1\ddot{u} + I_2\ddot{\varphi} \tag{7c}$$

where P_0 and q are respectively the axially and transversely applied loads; the stress resultants (N, M, Q, Y) and mass inertias (I_0, I_1, I_2) are defined by:

$$N = \int_A \sigma_{xx} dA \tag{8a}$$

$$M = \int_A z\sigma_{xx} dA \tag{8b}$$

$$Q = k\int_A \sigma_{xz} dA \tag{8c}$$

$$Y = \int_A m_{xy} dA \tag{8d}$$

$$(I_0, I_1, I_2) = \int_A (1, z, z^2)\rho dA \tag{9}$$

with k is the shear correction factor and ρ is the mass density.

2.2. Constitutive relations

Two types of sandwich beams as shown in Fig. 1 are considered in this study: (1) Type A: sandwich beams with an homogeneous core and FG skins and (2) Type B:

sandwich beams with a FG core and homogeneous skins. The material properties of the beam such as Young's modulus E, shear modulus G, Poisson's ratio ν and mass density ρ are assumed to vary continuously through the thickness. The effective material properties can be calculated using the Mori-Tanaka homogenization technique [13-14, 16-18]. Based on Mori-Tanaka homogenization scheme, the effective bulk modulus K_e and shear modulus G_e are given by [19]:

$$\frac{K_e - K_m}{K_c - K_m} = \frac{V_c}{1 + V_m \dfrac{K_c - K_m}{K_m + \frac{4}{3}G_m}} \tag{10a}$$

$$\frac{G_e - G_m}{G_c - G_m} = \frac{V_c}{1 + V_m \dfrac{G_c - G_m}{G_m + G_m \frac{9K_m + 8G_m}{6K_m + 12G_m}}} \tag{10b}$$

where V is the volume fraction of the phase materials; the subscripts m and c denote the metallic and ceramic phases, respectively. The effective Young's modulus and Poisson's ratio of a FG microbeam are related to K_e and G_e by:

$$E(z) = \frac{9K_eG_e}{3K_e + G_e} \tag{11a}$$

$$\nu(z) = \frac{3K_e - 2G_e}{6K_e + 2G_e} \tag{11b}$$

while the effective the mass density can be computed using the rule of mixture as:

$$\rho(z) = \rho_c V_c + \rho_m V_m \tag{12}$$

The volume fractions of the metal and ceramic constituents are related by:

$$V_m + V_c = 1 \tag{13}$$

According to the simple power law distribution, the volume fraction of the ceramic constituent V_c can be expressed as:

$$\begin{cases} V_c(z)=\left(\dfrac{z-h_0}{h_1-h_0}\right)^p & \text{for } z\in[h_0,h_1] \\ V_c(z)=1 & \text{for } z\in[h_1,h_2] \\ V_c(z)=\left(\dfrac{z-h_3}{h_2-h_3}\right)^p & \text{for } z\in[h_2,h_3] \end{cases} \tag{14}$$

for a sandwich beam with an homogeneous core and FG skins (type A), and

$$\begin{cases} V_c(z)=0 & \text{for } z\in[h_0,h_1] \\ V_c(z)=\left(\dfrac{z-h_1}{h_2-h_1}\right)^p & \text{for } z\in[h_1,h_2] \\ V_c(z)=1 & \text{for } z\in[h_2,h_3] \end{cases} \tag{15}$$

for a sandwich beam with a FG core and homogeneous skins (type B), where p is the power law index that governs the volume fraction gradation.

The linear elastic constitutive relations are:

$$\sigma_{xx}=E(z)\varepsilon_{xx} \tag{16a}$$

$$\sigma_{xz}=\frac{E(z)}{2\left[1+\nu(z)\right]}\gamma_{xz} \tag{16b}$$

$$m_{xy}=\frac{E(z)}{1+\nu(z)}\ell^2\chi_{xy} \tag{16c}$$

Substituting Eq. (16) into Eq. (8), the stress resultants can be expressed in terms of generalized displacements (u,w,φ) as:

$$N=A\frac{du}{dx}+B\frac{d\varphi}{dx} \tag{17a}$$

$$M=B\frac{du}{dx}+D\frac{d\varphi}{dx} \tag{17b}$$

$$Q=kA_s\left(\varphi+\frac{dw}{dx}\right) \tag{17c}$$

$$Y = \frac{1}{2} A_n \left(\frac{d\varphi}{dx} - \frac{d^2 w}{dx^2} \right) \tag{17d}$$

where

$$\left(A, B, D\right) = \int_A \left(1, z, z^2\right) E\left(z\right) dA \tag{18a}$$

$$A_s = \int_A \frac{E\left(z\right)}{2\left[1+\nu\left(z\right)\right]} dA \tag{18b}$$

$$A_n = \ell^2 \int_A \frac{E\left(z\right)}{2\left[1+\nu\left(z\right)\right]} dA = \ell^2 A_s \tag{18c}$$

It should be noted that the shear stress σ_{xz} computed from the constitutive equation Eq. (16b) violates the zero transverse shear stress conditions on the top and bottom surfaces of the beam, and thus requiring a shear correction factor. To avoid the use of the shear correction factor, equilibrium equations are used herein. Based on equilibrium equations, the transverse shear stress and shear force are given as follow [20]:

$$\sigma_{xz} = \tilde{m} Q \tag{19a}$$

$$Q = H\left(\varphi + \frac{dw}{dx} \right) \tag{19b}$$

The expressions for $\tilde{m}$ and H can be found in Nguyen et al. [20].

2.3. Analytical solutions

By substituting Eqs. (17) and (19) into Eq. (7), the governing equations of motion can be rewritten in terms of generalized displacements (u, w, φ) as:

$$A \frac{d^2 u}{dx^2} + B \frac{d^2 \varphi}{dx^2} = I_0 \ddot{u} + I_1 \ddot{\varphi} \tag{20a}$$

$$H\left(\frac{d\varphi}{dx} + \frac{d^2 w}{dx^2} \right) + \frac{A_n}{4} \left(\frac{d^3 \varphi}{dx^3} - \frac{d^4 w}{dx^4} \right) - P_0 \frac{d^2 w}{dx^2} + q = I_0 \ddot{w} \tag{20b}$$

$$B\frac{d^2u}{dx^2}+D\frac{d^2\varphi}{dx^2}-H\left(\varphi+\frac{dw}{dx}\right)+\frac{A_n}{4}\left(\frac{d^2\varphi}{dx^2}-\frac{d^3w}{dx^3}\right)=I_1\ddot{u}+I_2\ddot{\varphi} \tag{20c}$$

Based on Navier approach, the solutions of Eq. (20) for a simply supported beam are assumed as:

$$\begin{aligned} u(x,t)&=\sum_{n=1}^{\infty}U_n e^{i\omega t}\cos\alpha x \\ w(x,t)&=\sum_{n=1}^{\infty}W_n e^{i\omega t}\sin\alpha x \\ \varphi(x,t)&=\sum_{n=1}^{\infty}\phi_n e^{i\omega t}\cos\alpha x \end{aligned} \tag{21}$$

where $i=\sqrt{-1}$, $\alpha=n\pi/L$, and ω is the frequency of vibration. The transverse load q is also expanded in Fourier series as:

$$q(x)=\sum_{n=1}^{\infty}Q_n\sin\alpha x \tag{22}$$

where

$$Q_n=\begin{cases} q_0 & \text{for sinusoidal load of intensity } q_0 \\ \dfrac{4q_0}{n\pi} & \text{for uniform load of intensity } q_0 \end{cases} \tag{23}$$

Substituting Eqs. (21) and (22) into Eq. (20), the analytical solutions can be obtained from the following equations:

$$\left(\begin{bmatrix} k_{11} & 0 & k_{13} \\ 0 & k_{22} & k_{23} \\ k_{13} & k_{23} & k_{33} \end{bmatrix}-\alpha^2P_0\begin{bmatrix} 0 & 0 & 0 \\ 0 & 1 & 0 \\ 0 & 0 & 0 \end{bmatrix}-\omega^2\begin{bmatrix} m_{11} & 0 & m_{13} \\ 0 & m_{22} & 0 \\ m_{13} & 0 & m_{33} \end{bmatrix}\right)\begin{Bmatrix} U_n \\ W_n \\ \phi_n \end{Bmatrix}=\begin{Bmatrix} 0 \\ Q_n \\ 0 \end{Bmatrix} \tag{24}$$

where

$$\begin{aligned} &k_{11}=A\alpha^2,\ k_{13}=B\alpha^2,\ k_{22}=H\alpha^2+\frac{A_n}{4}\alpha^4,\ k_{23}=H\alpha-\frac{A_n}{4}\alpha^3,\ k_{33}=H+\left(D+\frac{A_n}{4}\right)\alpha^2 \\ &m_{11}=m_{22}=I_0,\ m_{13}=I_1,\ m_{33}=I_2 \end{aligned} \tag{25}$$

3. Numerical results and discussions

Unless mentioned otherwise, simply supported FG sandwich microbeams composed of aluminum Al ($E_m = 70\,\text{GPa}$, $\nu_m = 0.30$, $\rho_m = 2702\,\text{kg/m}^3$) and ceramic SiC ($E_c = 427$ GPa, $\nu_c = 0.17$, $\rho_c = 3100\,\text{kg/m}^3$) with length-to-thickness ratio $L/h = 10$ are considered. Since the material length scale parameter is not available for FG microbeams, it was assumed to be equal to $\ell = 15\,\mu\text{m}$ based on a reference value of a homogeneous epoxy beam [21]. Two type of FG sandwich microbeams with four different schemes including symmetric schemes (1-1-1) and (1-2-1) and non-symmetric schemes (2-1-1) and (2-2-1) were considered. The following dimensionless forms are used:

$$\begin{aligned} &\bar{w} = 100\frac{E_m h^3}{12 q_0 L^4} w\left(\frac{L}{2}\right),\ \bar{\sigma}_{xx}(z) = \frac{h}{q_0 L}\sigma_{xx}\left(\frac{L}{2}, z\right) \\ &\bar{\sigma}_{xz}(z) = \frac{h}{q_0 L}\sigma_{xz}(0, z),\ \bar{\omega} = \frac{\omega L^2}{h}\sqrt{\frac{\rho_m}{E_m}},\ \bar{P}_{cr} = \frac{12 P_0 L^2}{E_m h^3} \end{aligned} \tag{26}$$

3.1. Verification studies

So far there are no available results for FG sandwich microbeams. Therefore, in order to verify validity of the present results, two cases of verification were carried out: (1) FG microbeams with the size effect ($\ell \neq 0$) and (2) FG sandwich beams without the size effect ($\ell = 0$).

Tables 1 and 2 contain dimensionless deflections and fundamental frequencies of FG microbeams, respectively. The obtained results were compared with those reported by Simsek and Reddy [17] using the TBT. An excellent agreement between the results was found for all values of power law index p, dimensionless material length scale parameter h/ℓ and length-to-thickness ratio L/h. It is worth noting that the results given in Tables 1 and 2 were obtained based on the constitutive equations derived from a three-dimensional (3D) relation as:

$$\sigma_{xx} = \frac{E(z)\left[1-\nu(z)\right]}{\left[1+\nu(z)\right]\left[1-2\nu(z)\right]}\varepsilon_{xx} \tag{27}$$

To further verify the present results, Table 3 shows the comparison of dimensionless critical buckling loads predicted by the present work and Simsek and Reddy [18] using the TBT. For this comparison, the following material properties were used: steel SUS304 ($E_m = 210\,\text{GPa}$, $\nu_m = 0.3177$, $\rho_m = 8166\,\text{kg/m}^3$) and alumina Al_2O_3 ($E_c = 390$ GPa, $\nu_c = 0.3$, $\rho_c = 3960\,\text{kg/m}^3$). It can be seen that obtained results agree well with the solutions given by Simsek and Reddy [18] confirming the validity of the present results for the analysis of FG microbeams.

To verify for FG sandwich beams without the size effect ($\ell = 0$), a FG sandwich beam (type A) with the following material properties were considered: Aluminum Al ($E_m = 70$ GPa, $\nu_m = 0.3$, $\rho_m = 2702$ kg/m^3) and Alumina Al_2O_3 ($E_c = 380$ GPa, $\nu_c = 0.3$, $\rho_c = 3960\,\text{kg/m}^3$). In this verification, the effective material properties were evaluated using the rule of mixture. Dimensionless deflections, fundamental frequencies and critical buckling loads obtained in this study were compared with those generated by Vo et al. [22-23] using the TBT and HBT in Tables 4-6. Again, the obtained results are very close to the TBT solutions [22] and HBT solutions [23] for FG sandwich beams with different schemes and values of p and L/h.

3.2. Parameter studies

Parameter studies were carried out to investigate the effects of the material length scale parameter ℓ and power law index p on the deflection, stress, frequency and critical buckling load of simply supported FG sandwich microbeams. The results of both the present size-dependent model ($\ell \neq 0$) and classical model ($\ell = 0$) are given Tables 7-11 for two types of FG sandwich beams with different values of h/ℓ and p.

It can be observed from Tables 7-11 that, for the case of homogeneous beams ($p = 0$), all sandwich schemes give the same results for the type A but different results for the type B. This is due to the fact that when the power law index p was equal to 0, the volume fraction of the ceramic phase V_c will be equal to 1.0 for all layers of the type A (see Eq. (14)). Therefore, the type A sandwich beam behaves like an isotropic beam made of the ceramic constituent.

For the bending analysis, a FG sandwich microbeam subjected to uniform loads was considered. Dimensionless deflections, normal stresses and transverse shear stresses are respectively tabulated in Tables 7-9. The variations of the normal and transverse shear stresses through the thickness were also plotted in Figs. 2-5, whilst the variation of the deflection with respect to h/ℓ was illustrated in Fig. 6. In general, the inclusion of the size effect in the analysis ($\ell \neq 0$) results in reductions of both the deflection and stresses. These reductions become remarkably significant when the beam depth was small (e.g., $h = \ell$) and can be negligible when the beam depth was larger. This statement can be clearly seen in Fig. 6 where the size effect almost diminishes at the beam depth greater than twenty times the material length scale parameter ($h > 20\ell$). For the type A, the size effect of FG beams ($p \neq 0$) was more pronounced than the homogeneous one ($p = 0$) as indicated in Fig. 7 in which the deflection ratio was defined as the ratio of the deflection predicted by the classical model ($\ell = 0$) to that predicted by the present size-dependent model ($\ell \neq 0$).

As shown in Fig. 2(a) and Fig. 2(b), the distribution of the normal stress of the type A sandwich beams was symmetric through the middle plane for symmetric schemes (1-1-1) and (1-2-1) due to the symmetric configuration. It was also noticed from Fig. 2 that the maximum value of the normal stress in FG beams was not located at the top or bottom

surface of the beam as in the case of homogeneous beams. It is important to note that the transverse shear stress obtained in the present work was based on equilibrium equations (see Eq. (19)) and thus satisfying the stress-free boundary conditions on the top and bottom surfaces of the beam as shown in Figs. 4 and 5.

The effects of the material length scale parameter ℓ and power law index p on dimensionless fundamental frequencies are given in Table 10 and illustrated in Fig. 8. The results show that the dimensionless frequencies of the beam reduce by the increase of the beam depth, and this reduction is dramatic when $h < 5\ell$ and insignificant when $h > 10\ell$ (see Fig. 8). In other words, the effect of small scale on vibration behaviour is similar to that on bending behaviour, i.e. it is considerable only when the beam depth was at the micron scale. It is also observed from Table 10 and Fig. 8 that, for a constant beam depth, increasing the power law index p results in a reduction of dimensionless frequencies due to the low portion of ceramic in comparison with the metal phase as shown in Fig. 9. The effect of the material length scale parameter ℓ and power law index p on higher modes was plotted in Fig. 10 for the type A sandwich beams with the (1-1-1) scheme. In this figure, the frequency ratio was defined as the ratio of the frequency predicted by the present size-dependent model ($\ell \neq 0$) to that predicted by the classical model ($\ell = 0$). It is clearly seen from Fig. 10 that the effect of ℓ on frequency is similar for each mode.

Table 11 and Fig. 11 show the influences of the material length scale parameter ℓ and power law index p on the dimensionless critical buckling load. It can be seen that the variation of the critical buckling load with respect to ℓ and p exhibits similar trends with the variation of the frequency observed in the free vibration analysis. It means that the critical buckling load decrease with the increase of ℓ and p, and the

smaller the beam depth, the more significant the reduction.

4. Conclusions

Based on the modified couple stress theory and the TBT, the static bending, free vibration and buckling behaviours of FG sandwich microbeams have been investigated. The material properties of the FG sandwich microbeams which were assumed to vary continuously through the beam thickness were estimated using the Mori-Tanaka homogenization approach. Closed-form solutions for deflections, stresses, frequencies and critical buckling loads were presented for FG sandwich microbeams with simply supported boundary conditions. The validity of the present solutions has been verified for various case of with and without the material length scale parameter. Numerical results indicate that the inclusion of the small scale effect makes the beam stiffer, and consequently, leads to a reduction of both deflection and stresses and an increase in the critical buckling load and natural frequency. The small scale effect is remarkably significant at the micron scale and thus should be considered in the analysis of FG sandwich microbeams.

Acknowledgements

The authors gratefully acknowledge the financial support from the Basic Research Laboratory Program of the National Research Foundation of Korea (NRF) funded by the Ministry of Education, Science and Technology (2010-0019373 and 2012R1A2A1A01007405) and by Vietnam National Foundation for Science and Technology Development (NAFOSTED) under Grant No. 107.02-2012.07.

References

[1] Fu Y, Du H, Zhang S. Functionally graded TiN/TiNi shape memory alloy films.

Materials Letters 2003;57(20):2995-2999.

[2] Rahaeifard M, Kahrobaiyan MH, Ahmadian MT. Sensitivity analysis of atomic force microscope cantilever made of functionally graded materials. In: 3rd International Conference on Micro- and Nanosystems 2009;DETC2009-86254:539-544.

[3] Witvrouw A, Mehta A. The use of functionally graded poly-SiGe layers for MEMS applications. Materials Science Forum 2005;492-493:255-260.

[4] Chong ACM, Yang F, Lam DCC, Tong P. Torsion and bending of micron-scaled structures. Journal of Materials Research 2001;16(04):1052-1058.

[5] Fleck NA, Muller GM, Ashby MF, Hutchinson JW. Strain gradient plasticity: theory and experiment. Acta Metallurgica et Materialia 1994;42(2):475-487.

[6] Stolken JS, Evans AG. A microbend test method for measuring the plasticity length scale. Acta Materialia 1998;46(14):5109-5115.

[7] Yang F, Chong ACM, Lam DCC, Tong P. Couple stress based strain gradient theory for elasticity. International Journal of Solids and Structures 2002;39(10):2731-2743.

[8] Asghari M, Ahmadian MT, Kahrobaiyan MH, Rahaeifard M. On the size-dependent behavior of functionally graded micro-beams. Materials & Design 2010;31(5):2324-2329.

[9] Reddy JN. Microstructure-dependent couple stress theories of functionally graded beams. Journal of the Mechanics and Physics of Solids 2011;59(11):2382-2399.

[10] Nateghi A, Salamat-talab M, Rezapour J, Daneshian B. Size dependent buckling analysis of functionally graded micro beams based on modified couple stress theory. Applied Mathematical Modelling 2012;36(10):4971-4987.

[11] Akgoz B, Civalek O. Free vibration analysis of axially functionally graded tapered

Bernoulli–Euler microbeams based on the modified couple stress theory. Composite Structures 2013;98:314-322.

[12] Asghari M, Rahaeifard M, Kahrobaiyan MH, Ahmadian MT. The modified couple stress functionally graded Timoshenko beam formulation. Materials & Design 2011;32(3):1435-1443.

[13] Ke LL, Wang YS. Size effect on dynamic stability of functionally graded microbeams based on a modified couple stress theory. Composite Structures 2011;93(2):342-350.

[14] Simsek M, Kocaturk T, Akbas SD. Static bending of a functionally graded microscale Timoshenko beam based on the modified couple stress theory. Composite Structures 2013;95:740-747.

[15] Salamat-talab M, Nateghi A, Torabi J. Static and dynamic analysis of third-order shear deformation FG micro beam based on modified couple stress theory. International Journal of Mechanical Sciences 2012;57(1):63-73.

[16] Zhang B, He Y, Liu D, Gan Z, Shen L. Size-dependent functionally graded beam model based on an improved third-order shear deformation theory. European Journal of Mechanics - A/Solids 2014;47:211-230.

[17] Simsek M, Reddy JN. Bending and vibration of functionally graded microbeams using a new higher order beam theory and the modified couple stress theory. International Journal of Engineering Science 2013;64:37-53.

[18] Simsek M, Reddy JN. A unified higher order beam theory for buckling of a functionally graded microbeam embedded in elastic medium using modified couple stress theory. Composite Structures 2013;101:47-58.

[19] Mori T, Tanaka K. Average stress in matrix and average elastic energy of materials

with misfitting inclusions. Acta Metallurgica 1973;21(5):571-574.

[20] Nguyen TK, Vo TP, Thai HT. Static and free vibration of axially loaded functionally graded beams based on the first-order shear deformation theory. Composites Part B: Engineering 2013;55:147-157.

[21] Ansari R, Gholami R, Sahmani S. Free vibration analysis of size-dependent functionally graded microbeams based on the strain gradient Timoshenko beam theory. Composite Structures 2011;94(1):221-228.

[22] Vo TP, Thai HT, Nguyen TK, Inam F, Lee J. Static behaviour of functionally graded sandwich beams using a quasi-3D theory. Composites Part B: Engineering 2015;68:59-74.

[23] Vo TP, Thai HT, Nguyen TK, Maheri A, Lee J. Finite element model for vibration and buckling of functionally graded sandwich beams based on a refined shear deformation theory. Engineering Structures 2014;64:12-22.

Figure Captions

Fig. 1. Geometry and coordinate of a FG sandwich beam

Fig. 2. Variation of dimensionless normal stress $\bar{\sigma}_x$ across the thickness of FG sandwich beams under uniform loads ($p=1$, $L/h=10$, type A)

Fig. 3. Variation of dimensionless normal stress $\bar{\sigma}_x$ across the thickness of FG sandwich beams under uniform loads ($p=1$, $L/h=10$, type B)

Fig. 4. Variation of dimensionless transverse shear stress $\bar{\sigma}_{xz}$ across the thickness of FG sandwich beams under uniform loads ($p=1$, $L/h=10$, type A)

Fig. 5. Variation of dimensionless transverse shear stress $\bar{\sigma}_{xz}$ across the thickness of FG sandwich beams under uniform loads ($p=1$, $L/h=10$, type B)

Fig. 6. Effect of the material length scale parameter ℓ on the dimensionless deflection $\bar{w}$ of (1-2-1) FG sandwich beams under uniform loads ($p=1$, $L/h=10$)

Fig. 7. Effect of the power law index p on the deflections of FG sandwich beams under uniform loads (type A, $L/h=10$)

Fig. 8. Effects of the material length scale parameter ℓ and the power law index p on the dimensionless frequency $\bar{\omega}$ of (1-1-1) FG sandwich beams ($L/h=10$, type A)

Fig. 9. Variation of the volume fraction of the ceramic phase V_c across the thickness

Fig. 10. Effect of the material length scale parameter ℓ on higher frequencies of (1-1-1) FG sandwich beams ($L/h=10$, type A)

Fig. 11. Effects of the material length scale parameter ℓ and the power law index p on the dimensionless buckling load $\bar{P}_{cr}$ of (1-1-1) FG sandwich beams ($L/h=10$)

Table Captions

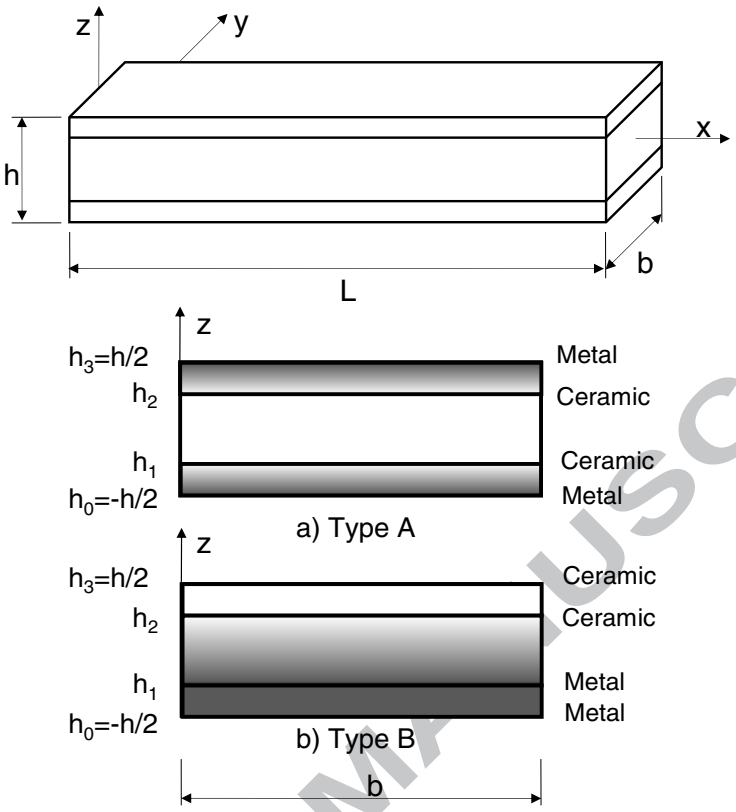

Fig. 1. Geometry and coordinate of a FG sandwich beam

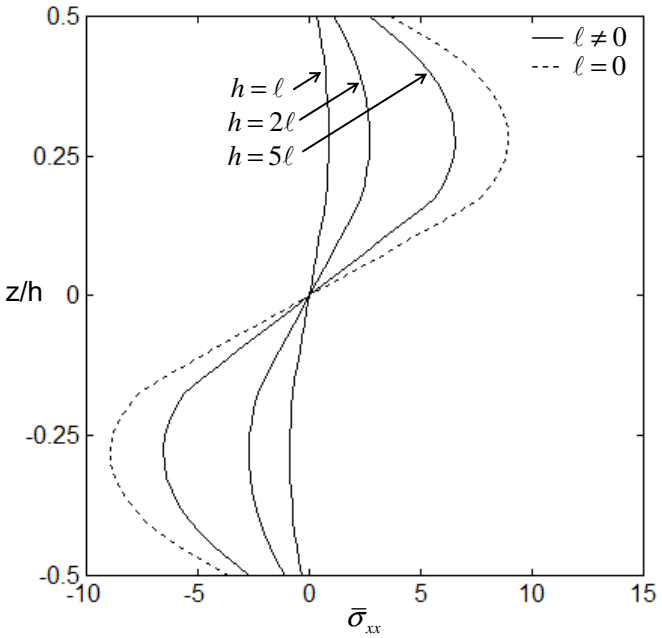

(a) Symmetric scheme (1-1-1)

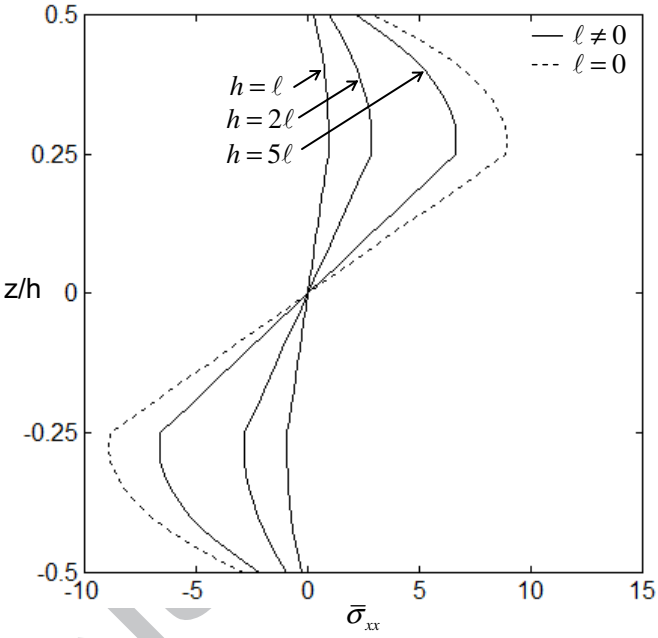

(b) Symmetric scheme (1-2-1)

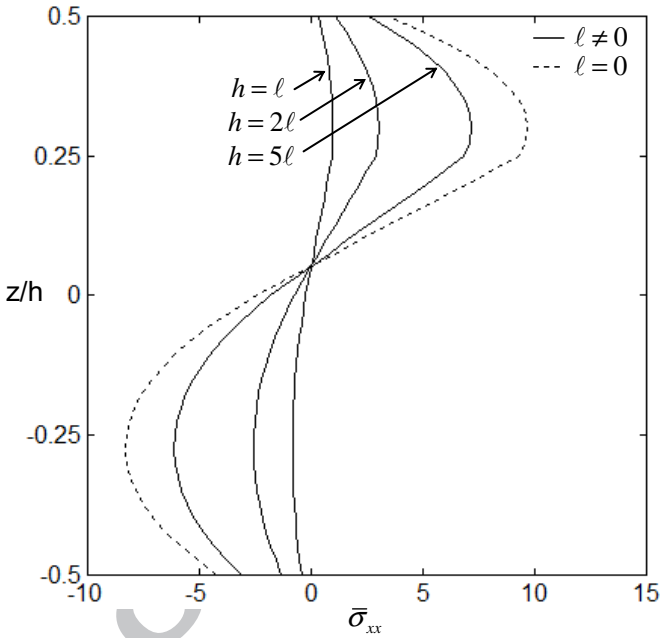

(c) Non-symmetric scheme (2-1-1)

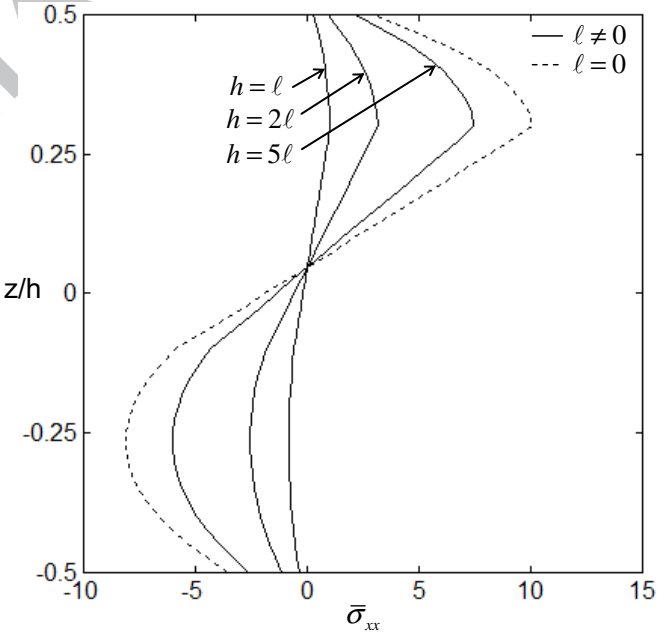

(d) Non-symmetric scheme (2-2-1)

Fig. 2. Variation of dimensionless normal stress $\bar{\sigma}_{xx}$ across the thickness of FG sandwich beams under uniform loads ($p = 1$, $L/h = 10$, type A)

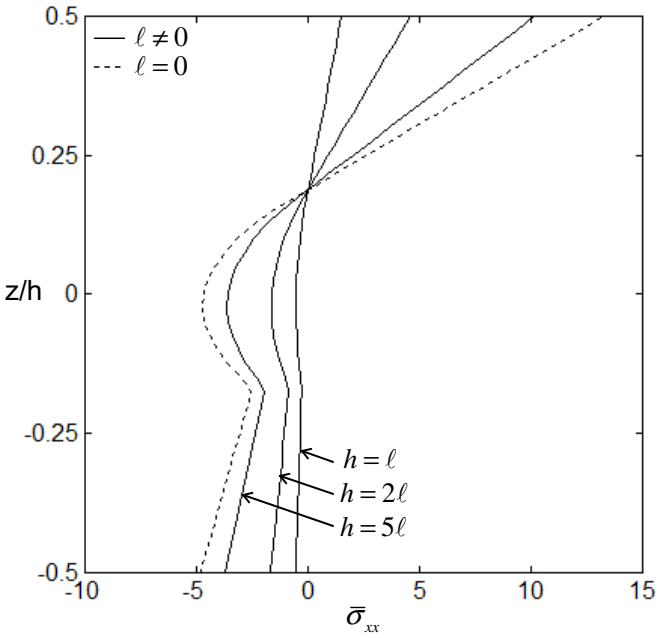

(a) Symmetric scheme (1-1-1)

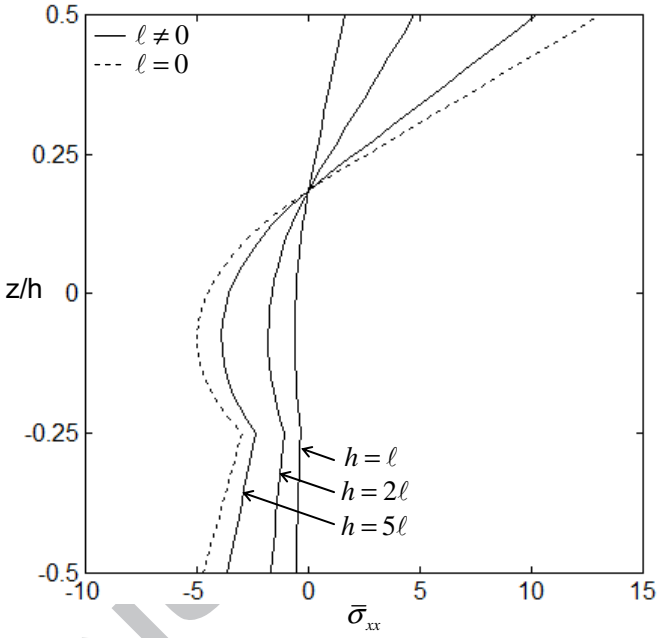

(b) Symmetric scheme (1-2-1)

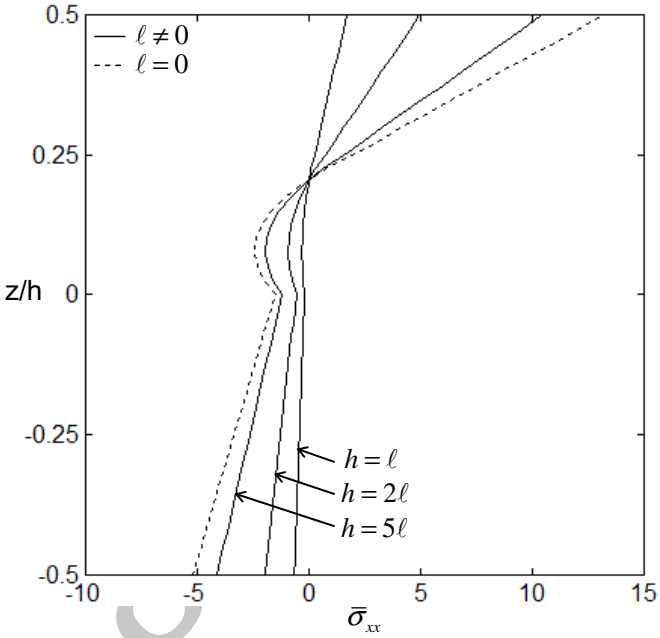

(c) Non-symmetric scheme (2-1-1)

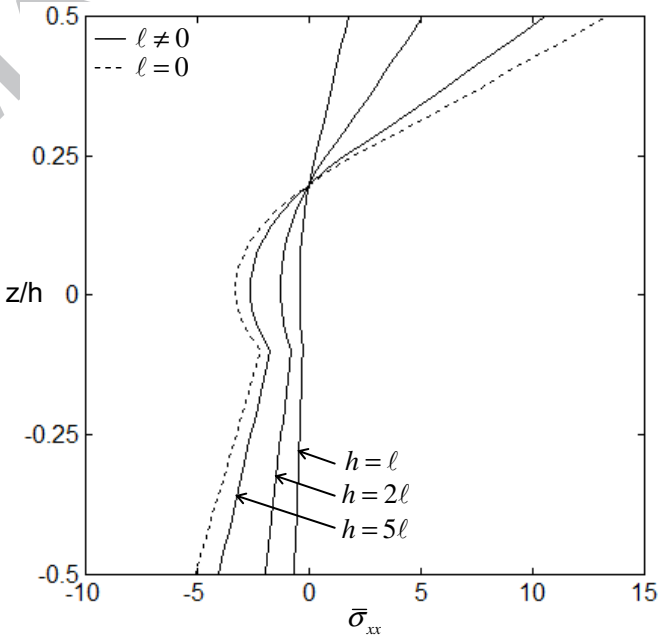

(d) Non-symmetric scheme (2-2-1)

Fig. 3. Variation of dimensionless normal stress $\bar{\sigma}_{xx}$ across the thickness of FG sandwich beams under uniform loads ($p = 1$, $L/h = 10$, type B)

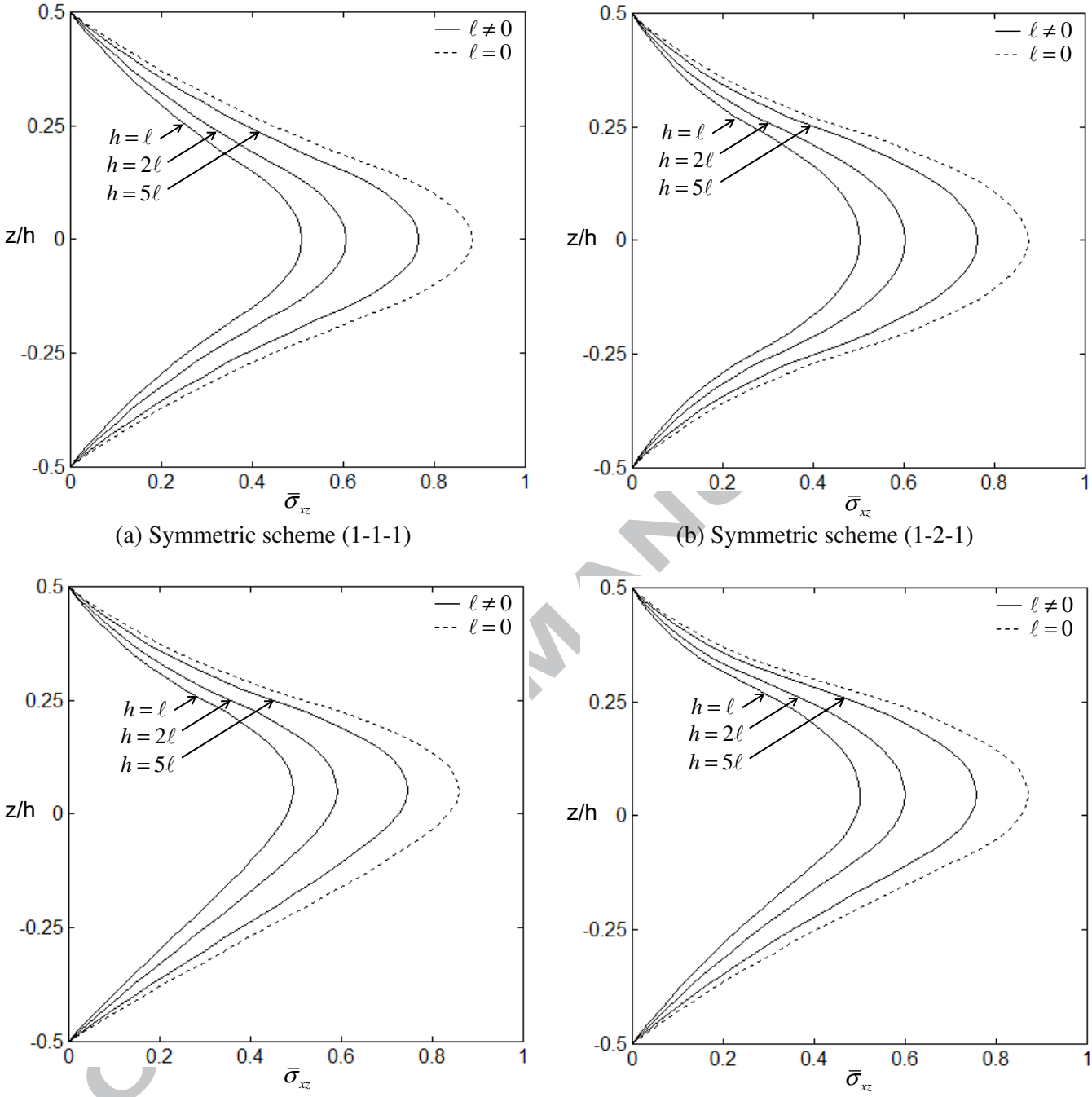

(a) Symmetric scheme (1-1-1)

(b) Symmetric scheme (1-2-1)

(c) Non-symmetric scheme (2-1-1)

(d) Non-symmetric scheme (2-2-1)

Fig. 4. Variation of dimensionless transverse shear stress $\bar{\sigma}_{xz}$ across the thickness of FG sandwich beams under uniform loads ($p = 1$, $L/h = 10$, type A)

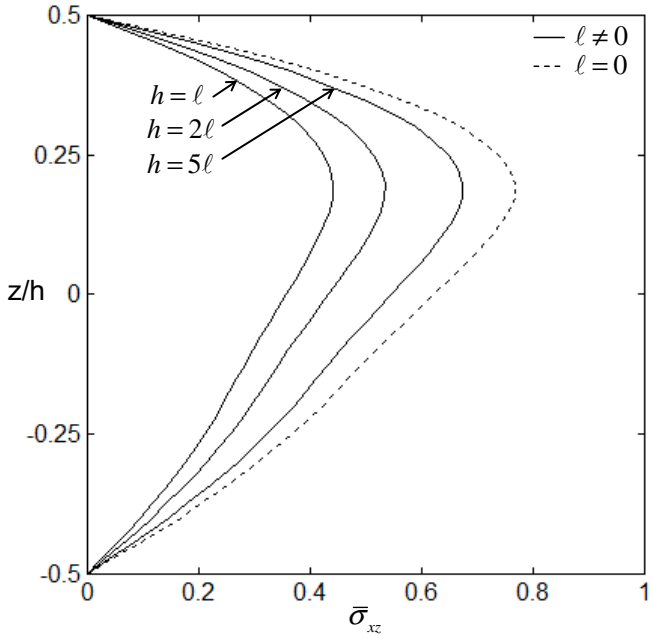

(a) Symmetric scheme (1-1-1)

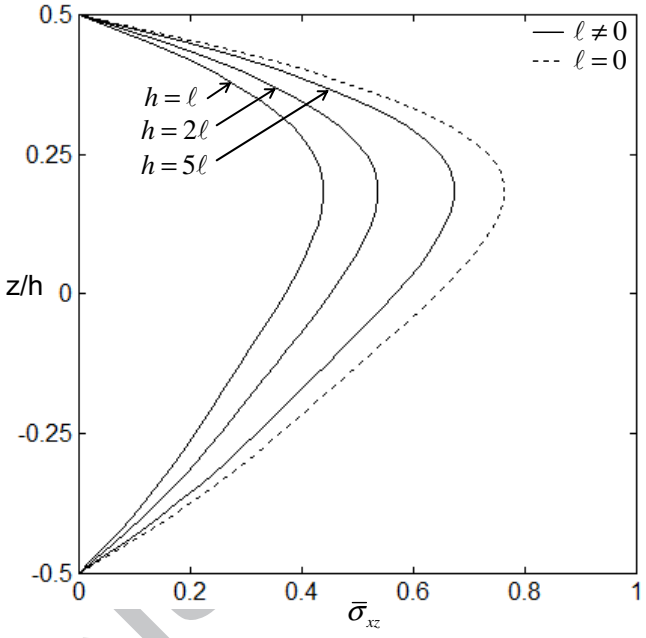

(b) Symmetric scheme (1-2-1)

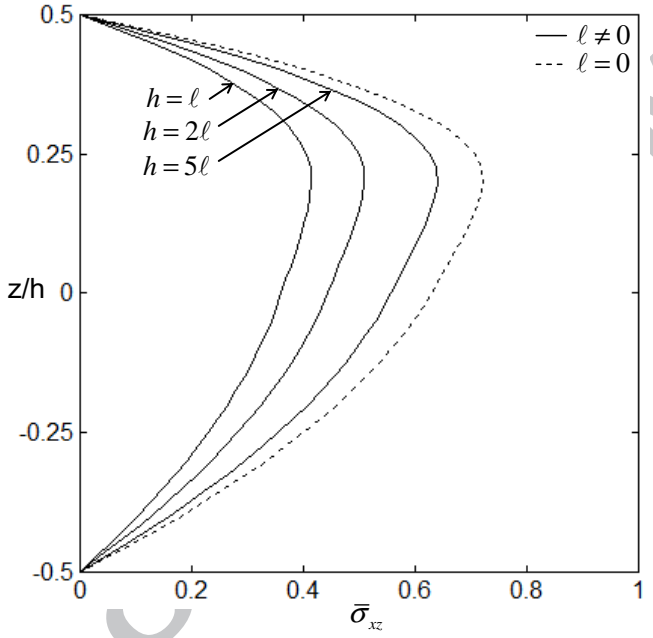

(c) Non-symmetric scheme (2-1-1)

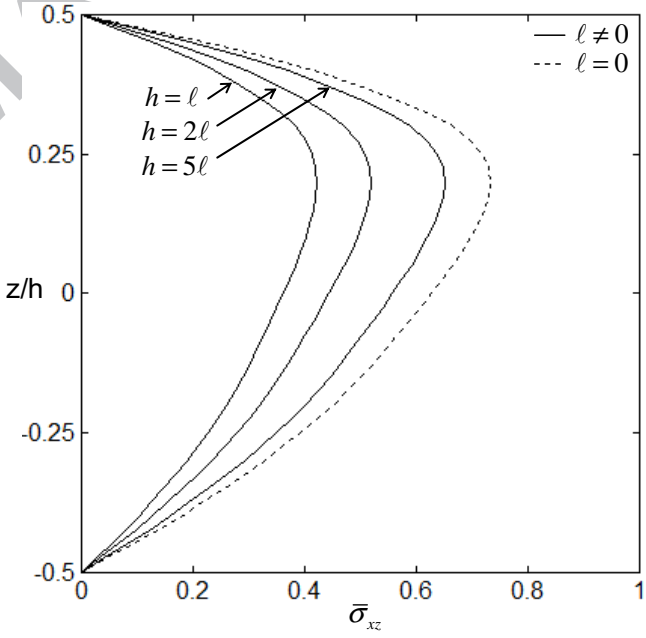

(d) Non-symmetric scheme (2-2-1)

Fig. 5. Variation of dimensionless transverse shear stress $\bar{\sigma}_{xz}$ across the thickness of FG sandwich beams under uniform loads ($p = 1$, $L / h = 10$, type B)

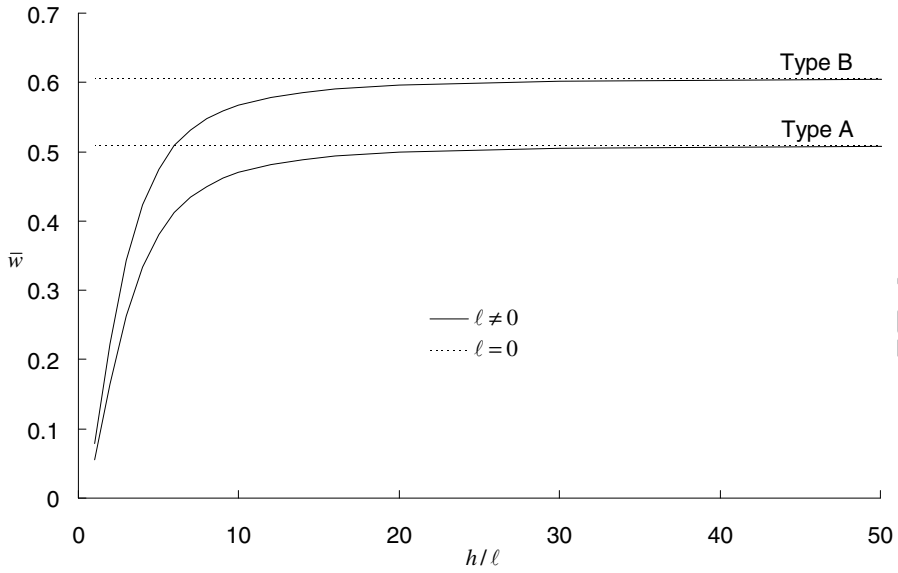

Fig. 6. Effect of the material length scale parameter ℓ on the dimensionless deflection $\bar{w}$ of (1-2-1) FG sandwich beams under uniform loads ($p = 1$, $L/h = 10$)

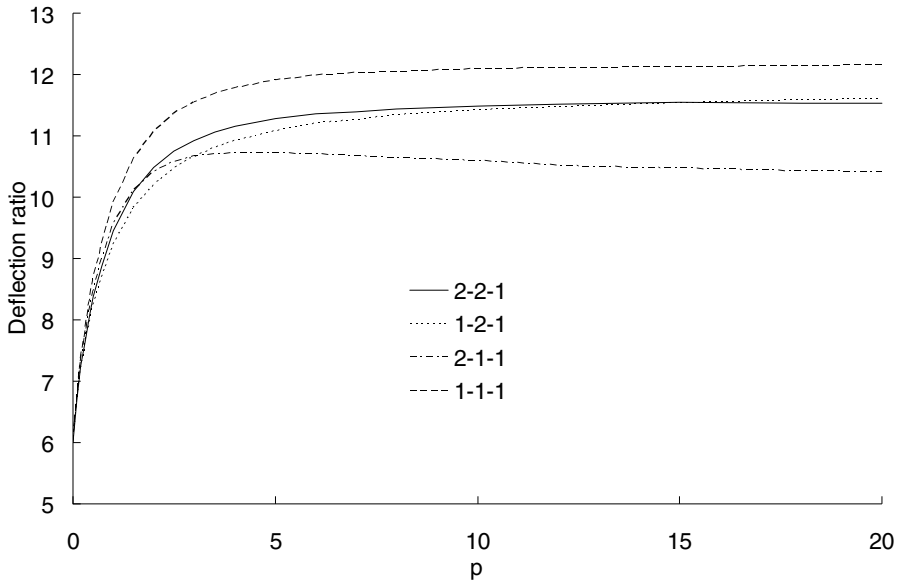

Fig. 7. Effect of the power law index p on the deflections of FG sandwich beams under uniform loads (type A, $L/h=10$)

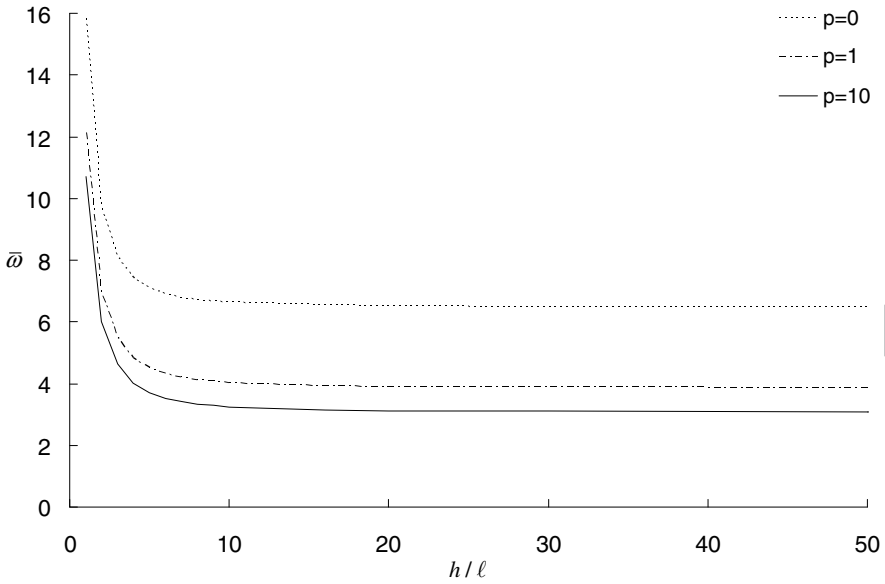

Fig. 8. Effects of the material length scale parameter ℓ and the power law index p on the dimensionless frequency $\bar{\omega}$ of (1-1-1) FG sandwich beams ($L/h=10$, type A)

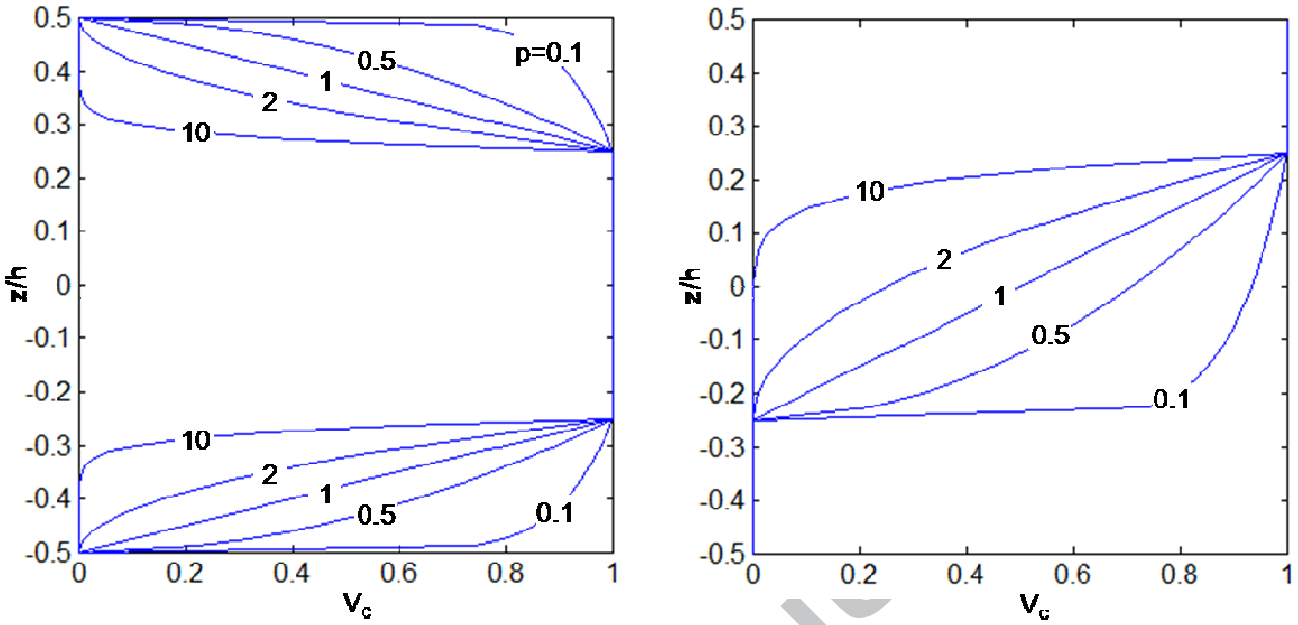

(a) Type A (b) Type B

Fig. 9. Variation of the volume fraction of the ceramic phase V_c across the thickness

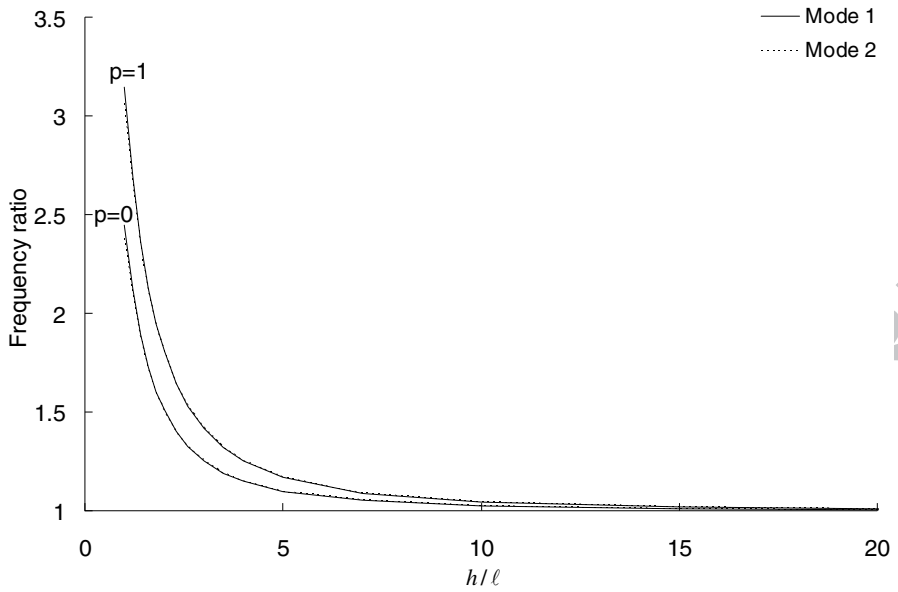

Fig. 10. Effect of the material length scale parameter ℓ on higher frequencies of (1-1-1) FG sandwich beams ($L/h=10$, type A)

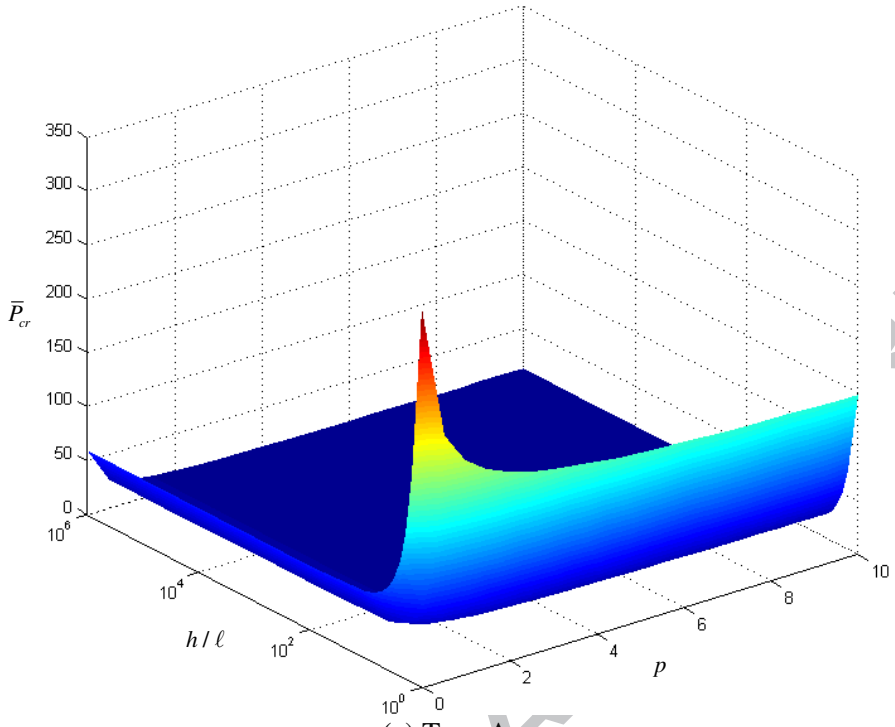

(a) Type A

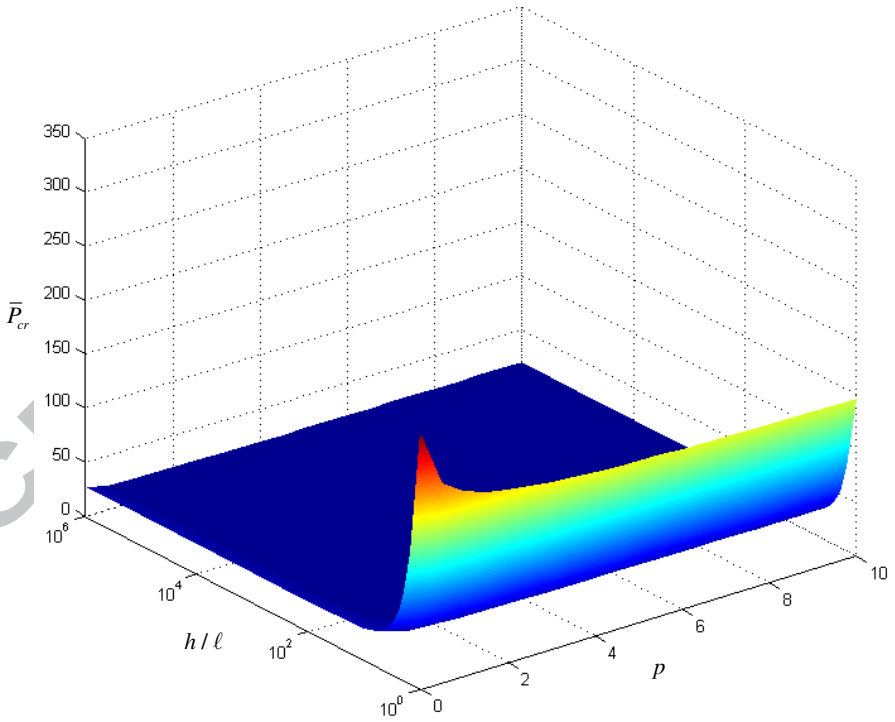

(b) Type B

Fig. 11. Effects of the material length scale parameter ℓ and the power law index p on the dimensionless buckling load $\bar{P}_{cr}$ of (1-1-1) FG sandwich beams ($L/h=10$)

Table 1. Dimensionless deflection $\bar{w}$ of FG microbeams under uniform loads

h/ℓ	Theory	$L/h=10$				$L/h=100$			
		$p=0.3$	1	3	10	$p=0.3$	1	3	10
1	TBT [17]	0.0592	0.0902	0.1330	0.1797	0.0565	0.0859	0.1262	0.1698
	Present	0.0594	0.0902	0.1330	0.1789	0.0567	0.0860	0.1262	0.1691
2	TBT [17]	0.1537	0.2292	0.3175	0.4095	0.1496	0.2228	0.3069	0.3940
	Present	0.1544	0.2293	0.3173	0.4058	0.1504	0.2228	0.3067	0.3902
4	TBT [17]	0.2603	0.3794	0.4928	0.6093	0.2543	0.3699	0.4778	0.5878
	Present	0.2620	0.3794	0.4925	0.6016	0.2559	0.3699	0.4774	0.5800
8	TBT [17]	0.3154	0.4542	0.5723	0.6946	0.3081	0.4430	0.5550	0.6702
	Present	0.3177	0.4542	0.5719	0.6845	0.3105	0.4430	0.5545	0.6601

Table 2. Dimensionless fundamental frequency $\bar{\omega}$ of FG microbeams

h/ℓ	Theory	$L/h=10$				$L/h=100$			
		$p=0.3$	1	3	10	$p=0.3$	1	3	10
1	TBT [17]	12.6058	10.3982	8.7110	7.5835	12.9533	10.6960	8.9820	7.8325
	Present	12.5893	10.3984	8.7145	7.6023	12.9355	10.6961	8.9856	7.8536
2	TBT [17]	7.8233	6.5211	5.6383	5.0237	7.9640	6.6461	5.7623	5.1442
	Present	7.8062	6.5212	5.6408	5.0473	7.9460	6.6463	5.7648	5.1697
4	TBT [17]	6.0115	5.0692	4.5256	4.1184	6.1096	5.1583	4.6187	4.2118
	Present	5.9931	5.0693	4.5275	4.1450	6.0904	5.1584	4.6207	4.2403
8	TBT [17]	5.4617	4.6327	4.1995	3.8573	5.5500	4.7135	4.2854	3.9444
	Present	5.4418	4.6329	4.2015	3.8857	5.5293	4.7136	4.2875	3.9747

Table 3. Dimensionless critical buckling load $\bar{P}_{cr}$ of FG microbeams ($L/h=20$)

h/ℓ	Theory	$p=0$	0.2	0.5	1	2	5	10	Metal
1	TBT [18]	101.7143	91.2490	82.5580	74.9674	68.1271	61.6033	58.4786	54.1609
	Present	101.6569	90.8166	82.4485	74.9253	68.0883	61.5695	58.4613	55.0508
2	TBT [18]	39.2016	34.9260	31.5537	28.7950	26.4790	24.2657	23.0415	20.9550
	Present	39.1884	34.7306	31.5064	28.7854	26.4701	24.2585	23.0436	21.5161
4	TBT [18]	23.4706	20.7526	18.7187	17.1759	15.9986	14.8699	14.1239	12.5989
	Present	23.4637	20.5807	18.6832	17.1709	15.9938	14.8665	14.1281	13.1204
8	TBT [18]	19.5314	17.2035	15.5047	14.2664	13.3741	12.5171	11.8909	10.5065
	Present	19.5257	17.0381	15.4722	14.2623	13.3702	12.5144	11.8953	11.0235

Table 4. Dimensionless deflection $\bar{w}$ of FG sandwich beams under uniform loads (type A)

p	Theory	$L/h=5$				$L/h=20$			
		1-1-1	1-2-1	2-1-1	2-2-1	1-1-1	1-2-1	2-1-1	2-2-1
0	TBT [22]	3.1657	3.1657	3.1657	3.1657	2.8963	2.8963	2.8963	2.8963
	Present	3.1657	3.1657	3.1657	3.1657	2.8962	2.8962	2.8962	2.8962
1	TBT [22]	6.3128	5.4408	6.5886	5.8749	5.9428	5.1024	6.2004	5.5182
	Present	6.2705	5.4135	6.5489	5.8418	5.9401	5.1007	6.1980	5.5162
2	TBT [22]	8.4582	6.8003	8.9597	7.6112	8.0356	6.4302	8.5047	7.2113
	Present	8.3962	6.7614	8.9098	7.5651	8.0317	6.4278	8.5018	7.2085
5	TBT [22]	11.3372	8.5762	11.9348	9.8720	10.8445	8.1681	11.3851	9.4170
	Present	11.2741	8.5269	11.9404	9.8327	10.8406	8.1650	11.3859	9.4149
10	TBT [22]	12.7006	9.4800	13.1433	10.9440	12.1677	9.0518	12.5362	10.4586
	Present	12.6708	9.4321	13.2483	10.9384	12.1658	9.0488	12.5433	10.4586

Table 5. Dimensionless fundamental frequency $\bar{\omega}$ of FG sandwich beams (type A)

p	Theory	$L/h=5$				$L/h=20$			
		1-1-1	1-2-1	2-1-1	2-2-1	1-1-1	1-2-1	2-1-1	2-2-1
0	HBT [23]	5.1528	5.1528	5.1528	5.1528	5.4603	5.4603	5.4603	5.4603
	Present	5.1525	5.1525	5.1525	5.1525	5.4603	5.4603	5.4603	5.4603
1	HBT [23]	3.8755	4.1105	3.8187	3.9896	4.0328	4.2889	3.9774	4.1602
	Present	3.8754	4.1103	3.8197	3.9909	4.0328	4.2889	3.9775	4.1602
2	HBT [23]	3.4190	3.7334	3.3514	3.5692	3.5389	3.8769	3.4754	3.7049
	Present	3.4178	3.7327	3.3510	3.5705	3.5388	3.8768	3.4754	3.7050
5	HBT [23]	3.0181	3.3771	2.9746	3.1928	3.1111	3.4921	3.0773	3.3028
	Present	3.0121	3.3747	2.9649	3.1902	3.1107	3.4919	3.0766	3.3026
10	HBT [23]	2.8808	3.2356	2.8669	3.0588	2.9662	3.3406	2.9662	3.1613
	Present	2.8692	3.2313	2.8467	3.0508	2.9654	3.3403	2.9647	3.1607

Table 6. Dimensionless critical buckling load $\bar{P}_{cr}$ of FG sandwich beams (type A)

p	Theory	$L/h=5$				$L/h=20$			
		1-1-1	1-2-1	2-1-1	2-2-1	1-1-1	1-2-1	2-1-1	2-2-1
0	HBT [23]	48.5959	48.5959	48.5959	48.5959	53.2364	53.2364	53.2364	53.2364
	Present	48.5904	48.5904	48.5904	48.5904	53.2363	53.2363	53.2363	53.2363
1	HBT [23]	24.5596	28.4447	23.5246	26.3611	25.9588	30.2307	24.8796	27.9540
	Present	24.5545	28.4375	23.5102	26.3540	25.9585	30.2303	24.8783	27.9533
2	HBT [23]	18.3587	22.7863	17.3249	20.3750	19.3116	23.9900	18.1404	21.3927
	Present	18.3430	22.7742	17.2845	20.3559	19.1989	23.9892	18.1372	21.3910
5	HBT [23]	13.7212	18.0914	13.0270	15.7307	14.2284	18.8874	13.5523	16.3834
	Present	13.6628	18.0624	12.8973	15.6638	14.2245	18.8854	13.5430	16.3783
10	HBT [23]	12.2605	16.3783	11.8370	14.1995	12.6819	17.0443	12.3084	14.7525
	Present	12.1562	16.3299	11.6216	14.0798	12.6749	17.0410	12.2931	14.7438

Table 7. Dimensionless deflection $\bar{w}$ of FG sandwich microbeams under uniform loads ($L/h=10$)

p	h/ℓ	Type A				Type B			
		1-1-1	1-2-1	2-1-1	2-2-1	1-1-1	1-2-1	2-1-1	2-2-1
0	1	0.0364	0.0364	0.0364	0.0364	0.0538	0.0485	0.0684	0.0589
	2	0.0960	0.0960	0.0960	0.0960	0.1586	0.1404	0.2007	0.1745
	5	0.1811	0.1811	0.1811	0.1811	0.3606	0.3085	0.4592	0.4023
	$\ell=0$	0.2183	0.2183	0.2183	0.2183	0.4771	0.4004	0.6105	0.5368
1	1	0.0648	0.0552	0.0707	0.0606	0.0752	0.0789	0.0912	0.0915
	2	0.1966	0.1645	0.2125	0.1816	0.2164	0.2233	0.2523	0.2523
	5	0.4704	0.3809	0.5005	0.4253	0.4757	0.4751	0.5215	0.5166
	$\ell=0$	0.6417	0.5095	0.6762	0.5727	0.6180	0.6065	0.6564	0.6471
2	1	0.0734	0.0598	0.0823	0.0673	0.0804	0.0878	0.0965	0.1003
	2	0.2279	0.1825	0.2520	0.2064	0.2292	0.2442	0.2630	0.2704
	5	0.5750	0.4434	0.6184	0.5079	0.4968	0.5079	0.5317	0.5357
	$\ell=0$	0.8120	0.6106	0.8577	0.7055	0.6409	0.6411	0.6621	0.6605
5	1	0.0824	0.0643	0.0953	0.0741	0.0856	0.0969	0.1016	0.1092
	2	0.2594	0.1996	0.2927	0.2307	0.2407	0.2636	0.2726	0.2874
	5	0.6777	0.5041	0.7292	0.5876	0.5131	0.5318	0.5402	0.5508
	$\ell=0$	0.9811	0.7126	1.0217	0.8358	0.6561	0.6611	0.6661	0.6688
10	1	0.0866	0.0662	0.1017	0.0773	0.0879	0.1010	0.1037	0.1132
	2	0.2736	0.2068	0.3112	0.2412	0.2457	0.2722	0.2768	0.2951
	5	0.7187	0.5292	0.7710	0.6195	0.5192	0.5402	0.5439	0.5573
	$\ell=0$	1.0471	0.7562	1.0767	0.8875	0.6605	0.6657	0.6676	0.6717

Table 8. Dimensionless normal stress $\bar{\sigma}_{xx}(h/2)$ of FG sandwich microbeams under uniform loads ($L/h=10$)

p	h/ℓ	Type A				Type B			
		1-1-1	1-2-1	2-1-1	2-2-1	1-1-1	1-2-1	2-1-1	2-2-1
0	1	1.1897	1.1897	1.1897	1.1897	1.3133	1.2799	1.4004	1.3430
	2	3.2581	3.2581	3.2581	3.2581	4.0266	3.8497	4.3489	4.1577
	5	6.2125	6.2125	6.2125	6.2125	9.2532	8.5471	10.1054	9.7009
	$\ell=0$	7.5000	7.5000	7.5000	7.5000	12.2679	11.1154	13.4723	12.9731
1	1	0.3534	0.2998	0.3437	0.2982	1.5050	1.5941	1.6810	1.7411
	2	1.1080	0.9255	1.0704	0.9259	4.5615	4.7380	4.9548	5.0826
	5	2.6760	2.1642	2.5460	2.1901	10.1676	10.2157	10.4212	10.5707
	$\ell=0$	3.6567	2.8994	3.4458	2.9543	13.2433	13.0729	13.1592	13.2776
2	1	0.4001	0.3256	0.3900	0.3249	1.5401	1.6692	1.7446	1.8534
	2	1.2858	1.0286	1.2411	1.0331	4.6518	4.9193	5.0863	5.3173
	5	3.2745	2.5223	3.0791	2.5673	10.2469	10.3913	10.4768	10.7144
	$\ell=0$	4.6321	3.4799	4.2790	3.5722	13.2566	13.1541	13.0918	13.2520
5	1	0.4470	0.3500	0.4391	0.3506	1.5744	1.7552	1.8089	1.9830
	2	1.4611	1.1256	1.4131	1.1348	4.7336	5.1052	5.2202	5.5833
	5	3.8577	2.8698	3.5674	2.9224	10.2791	10.4900	10.5474	10.9026
	$\ell=0$	5.5956	4.0640	5.0114	4.1654	13.1899	13.0937	13.0577	13.2919
10	1	0.4672	0.3601	0.4616	0.3615	1.5887	1.7977	1.8385	2.0465
	2	1.5383	1.1656	1.4901	1.1779	4.7730	5.2053	5.2799	5.7269
	5	4.0876	3.0130	3.7466	3.0610	10.2847	10.5345	10.5884	11.0218
	$\ell=0$	5.9673	4.3131	5.2514	4.3956	13.1423	13.0621	13.0613	13.3690

Table 9. Dimensionless transverse shear stress $\bar{\sigma}_{xz}(0)$ of FG sandwich microbeams under uniform loads ($L/h=10$)

p	h/ℓ	Type A				Type B			
		1-1-1	1-2-1	2-1-1	2-2-1	1-1-1	1-2-1	2-1-1	2-2-1
0	1	0.3334	0.3334	0.3334	0.3334	0.4550	0.3969	0.1189	0.5486
	2	0.4157	0.4157	0.4157	0.4157	0.5483	0.4814	0.1432	0.6593
	5	0.5375	0.5375	0.5375	0.5375	0.7322	0.6397	0.1920	0.8826
	$\ell=0$	0.5951	0.5951	0.5951	0.5951	0.8444	0.7314	0.2226	1.0225
1	1	0.4571	0.4066	0.5352	0.4462	0.4503	0.4594	0.1845	0.3896
	2	0.5450	0.4880	0.6401	0.5342	0.5465	0.5610	0.2267	0.4795
	5	0.7311	0.6525	0.8578	0.7153	0.7281	0.7435	0.2999	0.6324
	$\ell=0$	0.8527	0.7549	0.9970	0.8300	0.8353	0.8462	0.3404	0.7151
2	1	0.5174	0.4302	0.6646	0.4986	0.3432	0.3739	0.2092	0.2706
	2	0.6103	0.5114	0.7885	0.5911	0.4178	0.4588	0.2583	0.3352
	5	0.8224	0.6871	1.0612	0.7953	0.5563	0.6068	0.3406	0.4400
	$\ell=0$	0.9731	0.8048	1.2477	0.9350	0.6372	0.6885	0.3851	0.4947
5	1	0.6327	0.4634	0.9194	0.5965	0.2086	0.2421	0.2359	0.2460
	2	0.7410	0.5466	1.0884	0.7026	0.2551	0.2994	0.2923	0.3070
	5	1.0012	0.7367	1.4692	0.9484	0.3393	0.3946	0.3847	0.4008
	$\ell=0$	1.1984	0.8731	1.7361	1.1271	0.3876	0.4451	0.4331	0.4476
10	1	0.7220	0.4856	1.1073	0.6723	0.1974	0.2353	0.2484	0.2651
	2	0.8448	0.5711	1.3137	0.7911	0.2417	0.2917	0.3091	0.3315
	5	1.1423	0.7707	1.7746	1.0690	0.3214	0.3839	0.4063	0.4319
	$\ell=0$	1.3749	0.9203	2.0917	1.2765	0.3659	0.4299	0.4556	0.4792

Table 10. Dimensionless fundamental frequency $\bar{\omega}$ of FG sandwich microbeams

p	h/ℓ	Type A				Type B			
		1-1-1	1-2-1	2-1-1	2-2-1	1-1-1	1-2-1	2-1-1	2-2-1
0	1	15.8337	15.8337	15.8337	15.8337	13.3095	13.9514	11.9338	12.7753
	2	9.7550	9.7550	9.7550	9.7550	7.7532	8.1976	6.9657	7.4227
	5	7.1017	7.1017	7.1017	7.1017	5.1423	5.5301	4.6051	4.8888
	$\ell=0$	6.4696	6.4696	6.4696	6.4696	4.4704	4.8538	3.9939	4.2322
1	1	12.1351	13.0839	11.6506	12.5289	11.3842	11.1113	10.4206	10.3895
	2	6.9695	7.5771	6.7208	7.2352	6.7072	6.6030	6.2642	6.2541
	5	4.5053	4.9786	4.3793	4.7270	4.5238	4.5266	4.3567	4.3700
	$\ell=0$	3.8573	4.3050	3.7677	4.0735	3.9688	4.0063	3.8831	3.9046
2	1	11.4924	12.6357	10.8903	11.9664	11.0444	10.5946	10.1596	9.9653
	2	6.5213	7.2328	6.2251	6.8311	6.5419	6.3489	6.1534	6.0683
	5	4.1057	4.6407	3.9734	4.3548	4.4428	4.4022	4.3269	4.3110
	$\ell=0$	3.4550	3.9543	3.3738	3.6950	3.9117	3.9182	3.8771	3.8823
5	1	10.9287	12.2570	10.2074	11.4769	10.7472	10.1416	9.9337	9.5967
	2	6.1600	6.9553	5.8259	6.5064	6.4073	6.1459	6.0608	5.9139
	5	3.8109	4.3769	3.6906	4.0764	4.3878	4.3265	4.3050	4.2711
	$\ell=0$	3.1672	3.6813	3.1178	3.4179	3.8803	3.8801	3.8766	3.8759
10	1	10.6974	12.1076	9.9224	11.2763	10.6249	9.9559	9.8429	9.4459
	2	6.0190	6.8519	5.6722	6.3820	6.3524	6.0641	6.0233	5.8483
	5	3.7135	4.2828	3.6035	3.9823	4.3694	4.3037	4.2960	4.2553
	$\ell=0$	3.0766	3.5827	3.0492	3.3271	3.8740	3.8769	3.8775	3.8757

Table 11. Dimensionless critical buckling load $\bar{P}_{cr}$ of FG sandwich microbeams

p	h/ℓ	Type A				Type B			
		1-1-1	1-2-1	2-1-1	2-2-1	1-1-1	1-2-1	2-1-1	2-2-1
0	1	352.1681	352.1681	352.1681	352.1681	238.4427	264.7995	187.5531	217.8015
	2	133.7564	133.7564	133.7564	133.7564	80.9712	91.4812	63.9712	73.5868
	5	70.9041	70.9041	70.9041	70.9041	35.6265	41.6396	27.9689	31.9293
	$\ell=0$	58.8456	58.8456	58.8456	58.8456	26.9254	32.0791	21.0390	23.9291
1	1	198.0034	232.7431	181.5212	212.0386	170.7500	162.6654	140.6339	140.2876
	2	65.3473	78.0995	60.4408	70.7521	59.3321	57.5011	50.8881	50.8950
	5	27.3105	33.7239	25.6667	30.2047	26.9987	27.0317	24.6248	24.8576
	$\ell=0$	20.0200	25.2167	18.9987	22.4312	20.7814	21.1753	19.5633	19.8459
2	1	174.9327	214.6634	155.9268	190.8467	159.4940	146.2180	132.8920	127.8655
	2	56.3582	70.3748	50.9808	62.2289	56.0260	52.5701	48.8197	47.4753
	5	22.3426	28.9761	20.7741	25.2938	25.8502	25.2836	24.1493	23.9701
	$\ell=0$	15.8217	21.0393	14.9783	18.2112	20.0400	20.0309	19.3912	19.4410
5	1	155.7847	199.7249	134.6181	173.1709	149.8573	132.4253	126.2934	117.4541
	2	49.5236	64.3482	43.8866	55.6911	53.3383	48.7008	47.0837	44.6675
	5	18.9578	25.4867	17.6157	21.8645	25.0248	24.1451	23.7663	23.3079
	$\ell=0$	13.0950	18.0296	12.5728	15.3715	19.5728	19.4216	19.2729	19.1963
10	1	148.2080	193.8797	126.1824	166.1200	145.9418	126.9289	123.6547	113.2920
	2	46.9518	62.1277	41.2717	53.2486	52.2457	47.1620	46.3774	43.4920
	5	17.8752	24.2768	16.6616	20.7376	24.7292	23.7653	23.6035	23.0360
	$\ell=0$	12.2697	16.9894	11.9300	14.4756	19.4412	19.2861	19.2309	19.1108